



Molecular underpinnings of cytoskeletal cross-talk

Angela Oberhofer^{a,1}, Emanuel Reithmann^{b,c,1}, Peter Spieler^a, Willi L. Stepp^a, Dennis Zimmermann^d, Bettina Schmid^e, Erwin Frey^{b,c,2} , and Zeynep Ökten^{a,2} 

^aPhysik Department E22, Technische Universität München, D-85748 Garching, Germany; ^bArnold Sommerfeld Center for Theoretical Physics, Ludwig-Maximilians-Universität München, D-80333 München, Germany; ^cCenter for NanoScience, Department of Physics, Ludwig-Maximilians-Universität München, D-80333 München, Germany; ^dKoch Institute for Integrative Cancer Research, Massachusetts Institute of Technology, Cambridge, MA 02139; and ^eGerman Center for Neurodegenerative Diseases, D-81377 München, Germany

Edited by James A. Spudis, Stanford University School of Medicine, Stanford, CA, and approved January 21, 2020 (received for review October 16, 2019)

Cross-talk between the microtubule and actin networks has come under intense scrutiny following the realization that it is crucial for numerous essential processes, ranging from cytokinesis to cell migration. It is becoming increasingly clear that proteins long-considered highly specific for one or the other cytoskeletal system do, in fact, make use of both filament types. How this functional duality of “shared proteins” has evolved and how their coadaptation enables cross-talk at the molecular level remain largely unknown. We previously discovered that the mammalian adaptor protein melanophilin of the actin-associated myosin motor is one such “shared protein,” which also interacts with microtubules in vitro. In a hypothesis-driven in vitro and in silico approach, we turn to early and lower vertebrates and ask two fundamental questions. First, is the capability of interacting with microtubules and actin filaments unique to mammalian melanophilin or did it evolve over time? Second, what is the functional consequence of being able to interact with both filament types at the cellular level? We describe the emergence of a protein domain that confers the capability of interacting with both filament types onto melanophilin. Strikingly, our computational modeling demonstrates that the regulatory power of this domain on the microscopic scale alone is sufficient to recapitulate previously observed behavior of pigment organelles in amphibian melanophores. Collectively, our dissection provides a molecular framework for explaining the underpinnings of functional cross-talk and its potential to orchestrate the cell-wide redistribution of organelles on the cytoskeleton.

cytoskeleton | cross-talk | intracellular organization | whole-cell simulation | bottom-up reconstitution

Over the past decades it has become increasingly clear that the functional cross-talk between the microtubule and the actin components of the cytoskeleton underlies many essential cellular processes such as mitosis, cell migration, and intracellular cargo distribution (1–5). Consistent with this notion, well-known accessory proteins of the microtubule or the actin network systems have been found to interact with both filament types in vitro and in vivo (6–8). The underlying molecular principles of how these “shared proteins” establish and/or regulate cross-talk between the two cytoskeletal systems remain largely mysterious.

We previously discovered that one well-characterized protein of the actin cytoskeletal system—mammalian melanophilin from mouse (*MmMlph*)—is such a “shared protein,” as demonstrated by its interaction with microtubules in vitro (9). *MmMlph* was originally identified as an essential adaptor, recruiting the myosin Va (*MmMyoVa*) motor to the pigment-containing organelles or melanosomes via the Rab27a GTPase. This forms one of the few well-characterized motor–cargo complexes in vivo (10), the tripartite *MmRab27a/MmMlph/MmMyoVa* complex (Fig. 1A) (11–16). It is also well established that mammalian *MmMlph* interacts with actin filaments via its C terminus (11, 17, 18). We have recently shown that, in vitro, the dephosphorylated C-terminal filament-binding domain (FBD) of *MmMlph* clearly favored microtubules over actin filaments, while phosphorylation by the prototypical protein kinase A (PKA) restored its preference for actin (9). This competitive

interaction of *MmMlph*’s C-terminal FBD with the two filament types ultimately sufficed to regulate the track selection of its *MmMyoVa* motor within the tripartite complex at reconstituted microtubule–actin crossings in vitro (Fig. 1A).

By contrast, in the mammalian model dynamic switching of pigment organelles between the two cytoskeletal networks is physiologically irrelevant (4). To unmask the molecular underpinnings and the functional relevance of such *Mlph*-mediated track selection, here we turn to physiologically relevant model organisms and seek to answer two key questions. What is the molecular “origin” of *Mlph*’s regulatory power over its *MyoVa* motor? Moreover, is the capability of *Mlph* to force its actin-associated *MyoVa* onto the “wrong” track sufficient to give rise to functional cross-talk on the cellular scale?

Results and Discussion

We traced back the functional origins of *Mlph*-regulated track selection from mammals to early and lower vertebrates using the zebrafish and *Xenopus* as well-established in vivo models. Contrary to the mammalian model, these two model organisms are in fact proposed to make use of cross-talk in order to reversibly distribute their melanosome organelles in a PKA-regulated manner in melanophore cells (1, 19, 20) (Fig. 1B). The latter allows fish and amphibians to actively control their skin color, a fascinating trait that is lost in mammals. Despite these species-specific differences, however, previous in vivo studies implicated that early and lower

Significance

Long considered independent, the microtubule and actin network systems are now known to engage in functional cross-talk to drive essential cellular processes such as whole-cell migration, mitotic spindle positioning, or cell-wide organelle transport. However, molecular details of cytoskeletal cross-talk remain largely elusive. Here, we combine bottom-up reconstitution and theoretical approaches to systematically dissect the underlying mechanistic principles of cytoskeletal cross-talk using the example of cell-wide organelle transport. We show that a small regulatory protein domain is sufficient to establish cross-talk on the microscopic scale and prompt a global reorganization of organelles on the microtubule–actin cytoskeleton on the cellular scale. Indeed, this analytical approach can reproduce the previously observed redistribution of organelles in vivo with remarkable accuracy.

Author contributions: A.O., E.R., D.Z., B.S., E.F., and Z.Ö. designed research; A.O., E.R., P.S., D.Z., B.S., and E.F. performed research; W.L.S. contributed new reagents/analytic tools; A.O., E.R., P.S., W.L.S., D.Z., E.F., and Z.Ö. analyzed data; and A.O., E.R., E.F., and Z.Ö. wrote the paper.

The authors declare no competing interest.

This article is a PNAS Direct Submission.

Published under the PNAS license.

¹A.O. and E.R. contributed equally to this work.

²To whom correspondence may be addressed. Email: frey@lmu.de or zoekten@ph.tum.de.

This article contains supporting information online at <https://www.pnas.org/lookup/suppl/doi:10.1073/pnas.1917964117/-DCSupplemental>.

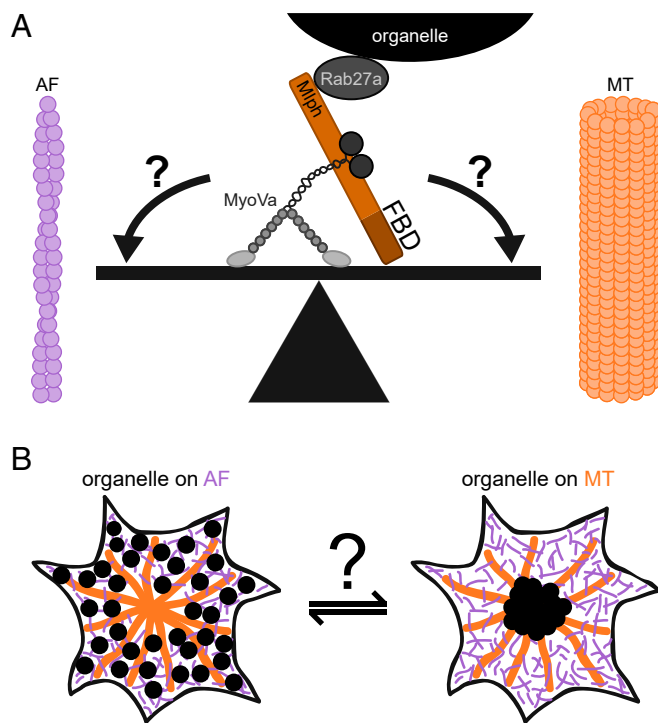


Fig. 1. (A) Illustration of the mammalian *MmRab27a/MmMlph/MmMyoVa* complex and the *MmMlph*-regulated track selection. To form the tripartite complex, the membrane-bound *MmRab27a* recruits the *MmMlph* adaptor in a guanosine triphosphate-dependent manner that in turn recruits the *MmMyoVa* motor to the surface of the organelle. Dependent on its phosphorylation state, the C-terminal FBD of *MmMlph* enforces a track selection by overriding the inherent preference of its *MmMyoVa* for actin filaments (AF), redirecting the motor onto microtubules (MT). (B) Illustration of the dynamic redistribution of melanosomes in melanophore cells that is proposed to be brought about by the functional cross-talk between the microtubule and actin network systems. As a result, organelles are toggled back and forth between the actin and microtubule networks. While the presumed Rab27a/Mlph/MyoVa tripartite complex ultimately enables dispersion on the actin network (Left), the minus-end-directed dynein motor aggregates the organelles in the cell center on the microtubules (Right). The underlying molecular principles of this proposed cross-talk between the two cytoskeletal systems are largely unknown.

vertebrates most likely use tripartite complexes homologous to those found on mammalian organelles to mediate motility on the cytoskeleton (1, 20, 21) (Fig. 1A). If true, the latter represents an unmatched opportunity to trace back the functional origins of Mlph-mediated track selection to early and lower vertebrates.

To directly test these hypotheses, we set out to reconstitute the presumed tripartite complexes from early and lower vertebrates using recombinantly expressed subunits to assess if they indeed form functional MyoVa-driven tripartite complexes. To this end, we turned to Rab27a, Mlph, and MyoVa homologs from zebrafish and *Xenopus*, respectively (SI Appendix, Fig. S1A; see SI Appendix for details). In particular, we expressed three different Mlph proteins from zebrafish with distinct C-terminal FBDs: *DrMlph-a*, *DrMlph-b* (paralog of *DrMlph-a*), and *DrMlph-bX2* (isoform of *DrMlph-b*), which most probably arose from a gene duplication event (SI Appendix, Fig. S1B) (21). We also expressed one isoform from *Xenopus*, as the functionally relevant FBDs are fully conserved among the respective isoforms (SI Appendix, Fig. S1C). To confirm that the Mlph homologs from zebrafish and *Xenopus* function as adaptor proteins for tripartite complex formation, as we had demonstrated previously with the mammalian *MmMlph* (Fig. 1A), we turned to single-molecule motility assays in vitro. Briefly, we labeled the respective Rab27a and MyoVa subunits

from zebrafish and *Xenopus* with two different fluorophores and followed their directional movement on surface-attached actin filaments in a TIRF (total internal reflection fluorescence) microscope. Only in the presence of Mlph (unlabeled) did Rab27a and the MyoVa motor move together along the filaments as part of a tripartite complex (Movies S1 and S2, Top). In the absence of Mlph, by contrast, the Rab27a subunit no longer displayed directional movement, and only the MyoVa motor moved along the actin filaments (Movies S1 and S2, Bottom). Together, our reconstitution assays demonstrate that the Mlph homologs from zebrafish and *Xenopus* function as an adaptor between the Rab27a and MyoVa subunits as described previously for the mammalian model (Fig. 1A).

We next screened the respective Mlph homologs from zebrafish and *Xenopus* for the functional phosphorylation sites that we had previously characterized in the mammalian model (9). Because the highly conserved phosphorylation site S498 in the mammalian FBD was also the most pronounced phosphorylation target in our in vitro assays (9), we focused our attention on the corresponding sites within the various FBDs from zebrafish and *Xenopus* (SI Appendix, Fig. S2A). While a corresponding site appeared to be present in the *Xenopus* *XtMlph* (S492), no such conserved recognition site for phosphorylation was evident in any of the zebrafish sequences (SI Appendix, Fig. S2A). Mass spectrometry analyses of in vitro-phosphorylated Mlph proteins, however, revealed several PKA-phosphorylated sites in the respective FBDs from zebrafish and *Xenopus* (SI Appendix, Fig. S2A and Tables S1–S4). Importantly, and in agreement with our previous findings with the mammalian *MmMlph* (9), phosphorylation and dephosphorylation of the Mlph proteins from zebrafish and *Xenopus* had no effect on the velocity and processivity of the respective MyoVa motors in the tripartite complexes (SI Appendix, Table S5). Having verified the functional integrity of the respective phosphorylated and dephosphorylated Mlph homologs, we next assessed their role in regulating track selection at reconstituted microtubule–actin crossings.

Melanophilin Proteins from Zebrafish Fail to Mediate Track Selection In Vitro.

First, we investigated whether the Mlph homologs from zebrafish and *Xenopus* are able to interact with microtubules and actin filaments in a phosphorylation-dependent manner in vitro. To this end, we attached both microtubules and actin filaments (labeled with two different fluorophores) to a glass coverslip and used a three-color TIRF microscope to probe the binding capability of the Rab27a/Mlph complexes (labeled with a third fluorophore on the Rab27a subunit) to the respective filaments. While the amphibian *XtMlph* interacted readily with both filament types (SI Appendix, Fig. S2B), all Mlph proteins from zebrafish (*DrMlph-a*, *DrMlph-b*, and *DrMlph-bX2*) failed to interact with microtubules (SI Appendix, Fig. S2C–E). Only *DrMlph-bX2* interacted with actin filaments (SI Appendix, Fig. S2C), but not *DrMlph-a* or *DrMlph-b* (SI Appendix, Fig. S2D and E).

The failure of the zebrafish *DrMlph* proteins to directly interact with microtubules raised the question of whether these proteins are at all able to regulate the track selection of their *DrMyoVa* motor at microtubule–actin crossings in vitro. To visualize the behavior of the respective tripartite complexes in a TIRF microscope, we labeled the Rab27a subunit, together with the microtubules and actin filaments, with three different fluorophores. In this way, a tripartite complex will either move directionally toward the barbed end of actin filaments (22) or display one-dimensional diffusion on microtubules as demonstrated previously (9, 23, 24). We then monitored whether or not, upon arrival at a crossing, a given complex would switch from one to the other filament type, or would simply ignore the crossing and continue on its way (SI Appendix, Fig. S3A and Movie S3). In stark contrast to our previous findings with the mammalian complex (9), the switching behavior of the phosphorylated and dephosphorylated complexes

from zebrafish at microtubule–actin crossings was essentially indistinguishable (Fig. 2 *A* and *A'* and *SI Appendix*, Fig. S3 *B–C'*). In fact, the zebrafish complexes largely reproduced the switching behavior of the unregulated mammalian tripartite complex that lacked its regulatory FBD (9). Together, these results show that the *DrMlph* proteins from zebrafish are unable to regulate the switching behavior of the *DrMyoVa*-based tripartite complex at cytoskeletal crossings in vitro. Indeed, the zebrafish *DrMyoVa* motor alone behaved in essentially the same way irrespective of whether or not *DrMlph* was present and faithfully replicated the switching behavior of the respective zebrafish complexes (*SI Appendix*, Fig. S3 *D* and *D'*). Because none of the zebrafish *DrMlph* proteins were able to regulate track selection at microtubule–actin crossings, we decided to investigate whether it is possible to engineer a “regulatable” zebrafish complex.

Engineering Regulated Track Selection In Vitro. It is conceivable that the mammalian *MmMyoVa* complex has evolved specific features to enable a regulatory control of the *MmMlph* adaptor over

its *MmMyoVa* motor that may not yet exist in the early vertebrate zebrafish. If, however, the FBD-mediated regulation is autonomous, the sole presence of the mammalian FBD will be expected to prompt a PKA-dependent response from the unresponsive zebrafish complex at microtubule–actin crossings.

To test this hypothesis, we fused the last ~100 residues of the mammalian FBD containing the S498 phosphorylation site to the zebrafish *DrMlph*-b (*SI Appendix*, Fig. S24; see *SI Appendix* for details). The presence of this distantly related mammalian FBD alone was sufficient to confer a capacity for phosphorylation-regulated switching at reconstituted microtubule–actin crossings onto the zebrafish complex. This behavior resembled that of the mammalian complex remarkably well (Fig. 2 *B*, *B'*, *D*, and *D'*) (9). Compared to the unregulated zebrafish complex, which switched with essentially the same probabilities from microtubules onto actin filaments irrespective of its phosphorylation state (Fig. 2*A*, Phos. vs. Dephos.), the switching probabilities of the chimeric complex containing the mammalian FBD differed substantially between phosphorylated and dephosphorylated states (Fig. 2*B*, Phos. vs. Dephos.). Strikingly, the

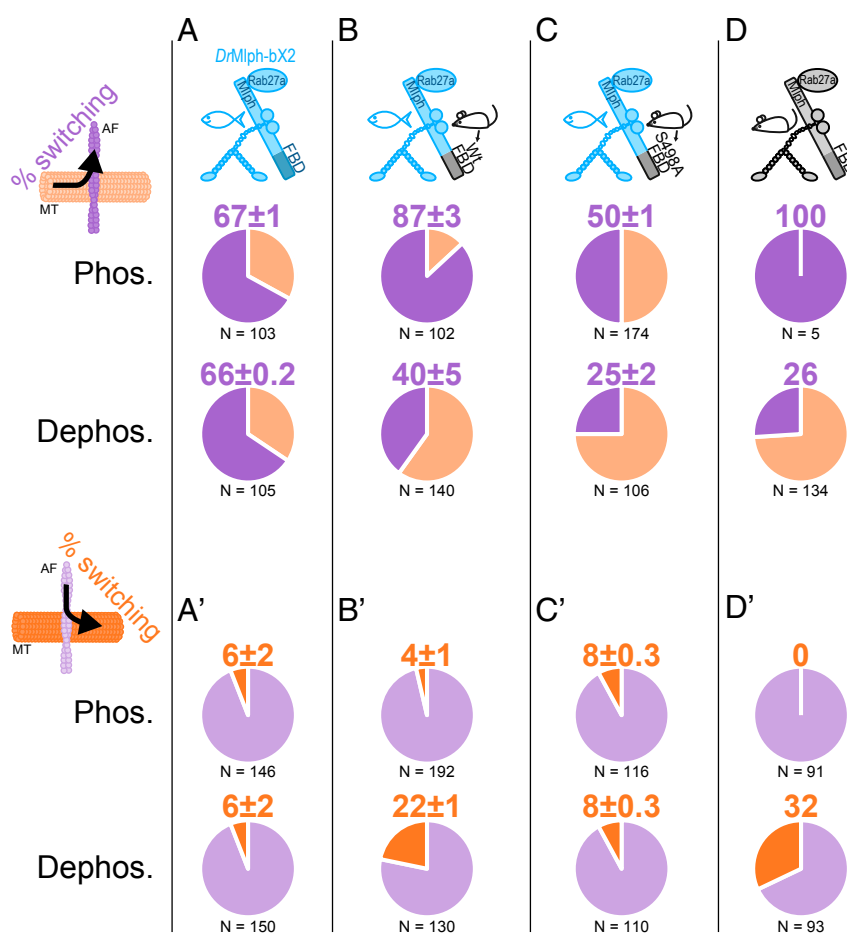


Fig. 2. (Top) Illustration of tripartite complexes employed in experiments. Left column: Respective switching directions and phosphorylation states (Phos. and Dephos.) of the complexes. Values (mean over experiments \pm SD) above the pie charts represent the color-coded switching probabilities in percent that correspond to the switching direction (Left). (A and A') The respective switching probabilities of the zebrafish tripartite complex assembled with the *DrMlph*-bX2 protein showed no dependence on *DrMlph*'s phosphorylation state (compare respective values for Phos. vs. Dephos.), largely recapitulating the switching behaviors shown in *SI Appendix*, Fig. S3. (B and B') When the mammalian FBD was fused to the zebrafish *DrMlph*-b, switching of the chimeric complex onto actin increased upon phosphorylation and decreased upon dephosphorylation (B, 87% for Phos. vs. 40% for Dephos.) relative to the unregulated wild-type zebrafish complex (A, ~66% for Phos. and Dephos.). (B') Dephosphorylation increased the switching of the chimeric complex onto microtubules approximately fivefold from 4 to 22% (B', Phos. vs. Dephos.). (C) Preventing PKA-dependent phosphorylation of the S498 significantly suppressed the switching onto actin (B vs. C, Phos. states) as expected, while dephosphorylation still efficiently suppressed the switching onto actin (B vs. C, Dephos. states). (C') The point mutation S498A abolished the capability to up-regulate switching onto microtubules (B' vs. C'), reproducing the behavior of the unregulated zebrafish complex (A' vs. C'). *n* = number of events from three independent sets of experiments. (D and D') Switching probabilities of the mammalian complex to facilitate comparison (replotted from ref. 9). AF, actin; MT, microtubule.

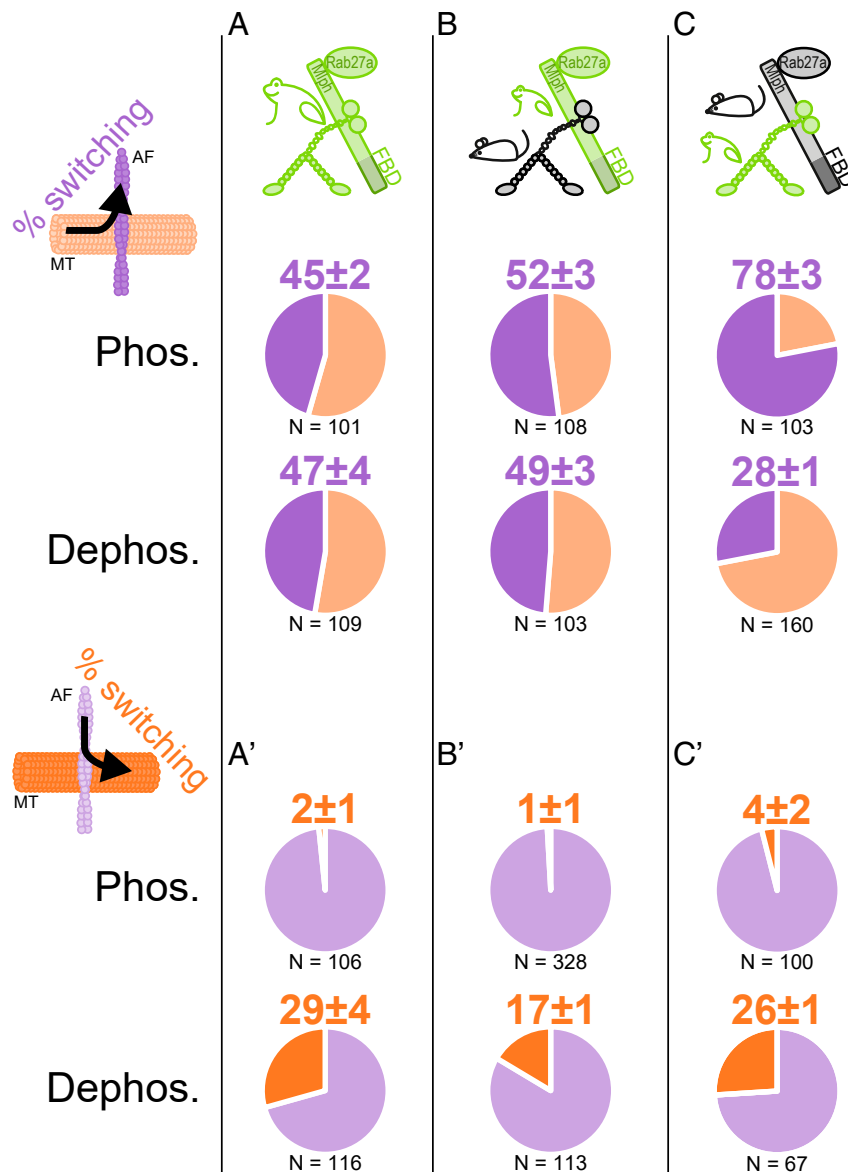


Fig. 3. Amphibian XtMlph regulates cross-talk at microtubule–actin crossings (for a description of illustrations on the left see Fig. 2). (A) Phosphorylated and dephosphorylated *Xenopus* complexes displayed largely indistinguishable switching behaviors from actin filaments onto microtubules (Phos. vs. Dephos.). (A') Upon dephosphorylation, the complex displayed a considerably enhanced switching from actin filaments onto microtubules (Phos. vs. Dephos.). (B) The mammalian *MmMyoVa* motor under the regulatory control of the amphibian XtMlph displayed a substantially reduced switching from ~100% (9) to ~50%, largely recapitulating the behavior of the amphibian *XtMyoVa* (A). (B') The switching from actin onto microtubules, on the other hand, was enhanced under the regulatory control of the amphibian XtMlph as previously observed with its mammalian homolog. (C) The surprisingly low switching probabilities of the amphibian complex to switch onto its actin filament have been significantly increased when the amphibian *XtMyoVa* switched under the control of the phosphorylated mammalian *MmMlph* (compare A vs. C, Top). Moreover, as observed with the mammalian complex (Fig. 2D), dephosphorylation also suppressed the switching of the complex onto actin filaments (compare C vs. Fig. 2D, Bottom). Therefore, the switching behavior of the amphibian *XtMyoVa* under the regulatory control of the mammalian *MmMlph* resembled the mammalian complex as shown in Fig. 2D rather than the amphibian complex (A). (C') As expected, the mammalian *MmMlph* was capable of enhancing the switching of the amphibian *XtMyoVa* onto microtubules upon dephosphorylation (compare C' vs. Fig. 2D'). *n* = number of events from three independent experiments for A and A' and two independent experiments for B to C'. AF, actin; MT, microtubule.

presence of the mammalian FBD alone sufficed to force the zebrafish *DrMyoVa* motor onto the “wrong” track, by significantly up-regulating the switching of the chimeric complexes from actin filaments onto microtubules upon dephosphorylation (Fig. 2B', Phos. vs. Dephos.). We were able to eliminate this up-regulation by replacing the S498 phosphorylation site with a nonphosphorylatable alanine (S498A) (Fig. 2C', Phos. vs. Dephos.).

This result underscores the regulatory dominance of the conserved serine residue S498 and suggests that incorporation of only a few functional phosphorylation sites may in fact suffice to

regulate track selection at microtubule–actin crossings in vitro. The fact that the zebrafish *DrMlph* proteins lack the ability to simultaneously interact with microtubules and actin filaments suggests that at least this particular early vertebrate cannot up-regulate the microtubule preference of its associated *DrMyoVa* motor. Contrary to zebrafish, the amphibian *XtMlph*, which appeared later in evolution, is capable of interacting with both filament types. This suggests that the amphibian *XtMlph* may in fact be capable of regulating the switching behavior of its *XtMyoVa* motor at microtubule–actin crossings.

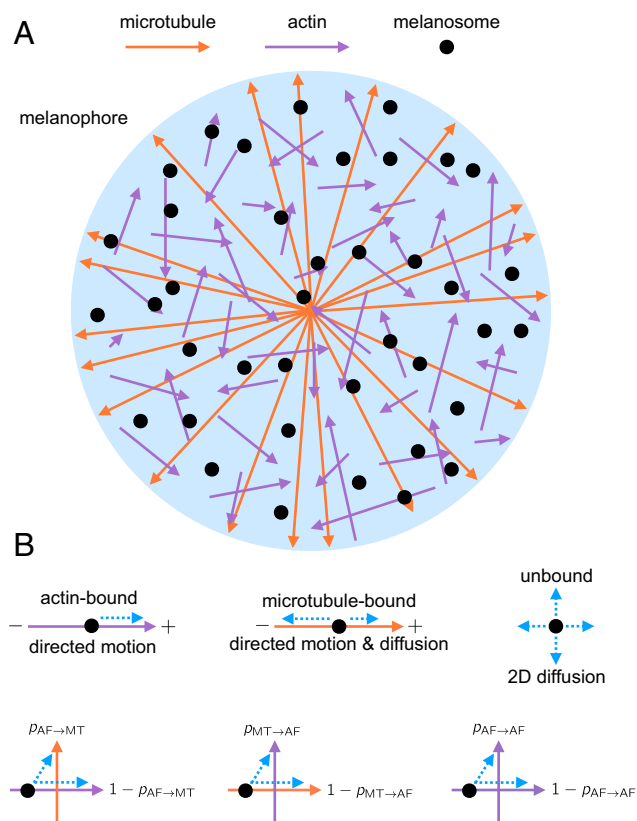


Fig. 4. Illustration of the computational (in silico) model. (A) Melanophores were modeled as two-dimensional circular cells (radius 30 μm) that contained straight actin filaments and microtubules with an intrinsic orientation (indicated by the arrows). The distribution of actin filaments was assumed to be homogeneous and isotropic in both position and orientation. The lengths were chosen from an exponential distribution (mean 1.5 μm). Microtubules were arranged radially (length $\sim 30 \mu\text{m}$) and extended from the center of the cell (minus ends) to the periphery (plus ends). (B) The dynamics of melanosomes (Top) were assumed to be directed toward the barbed end when bound to actin filaments, bidirectionally but with a bias toward the minus end when bound to microtubules, and diffusive in two dimensions when unbound. (Bottom) At any given crossing between filaments, melanosomes could either continue to move along the same filament or switch onto the other filament with respective switching probabilities $p_{AF \rightarrow MT}$, $p_{MT \rightarrow AF}$, and $p_{AF \rightarrow AF}$ (blue arrows indicate direction of movement). For further details on the model and its robustness, see *SI Appendix*, Table S6 and Figs. S6–S9. AF, actin; MT, microtubule.

Amphibian XtMlph Regulates Cross-Talk at Microtubule–Actin Crossings. As observed with the zebrafish complexes (Fig. 2A and *SI Appendix*, Fig. S3 B and C, Phos. vs. Dephos.), phosphorylated and dephosphorylated complexes from *Xenopus* switched with largely indistinguishable probabilities from microtubules onto actin filaments (Fig. 3A, Phos. vs. Dephos.). Strikingly, however, switching in the opposite direction—from actin filaments onto microtubules—was significantly increased upon dephosphorylation, which we had not observed with the zebrafish complexes (Fig. 3A', Phos. vs. Dephos., Fig. 2A', and *SI Appendix*, Fig. S3 B' and C', Phos. vs. Dephos.). Consistent with its role of regulating the track selection of its XlMyoVa motor, removal of the FBD abolished this up-regulation (*SI Appendix*, Fig. S4A', Phos. vs. Dephos.). Interestingly, when compared to the phosphorylated mammalian complex that switched onto the actin filament at microtubule–actin crossings with a probability of $\sim 100\%$ (Fig. 2D, Phos.) (9), $\sim 50\%$ of the amphibian complexes did not switch onto the actin filament and continued on the microtubule (Fig. 3A, Phos.). To gain a further

understanding of this considerable difference between the amphibian and mammalian tripartite complexes (Fig. 2D and D' vs. Fig. 3A and A'), we investigated whether it is the Mlph adaptor or the MyoVa motor that dominates the switching behavior at microtubule–actin crossings. To this end, we characterized the switching of the mammalian *MmMyoVa* under the regulatory control of the amphibian XlMlph and the amphibian XlMyoVa under the control of the mammalian *MmMlph*. Remarkably, the mammalian *MmMyoVa* under the control of the amphibian XlMlph largely reproduced the switching behavior of the amphibian XlMyoVa (Fig. 3B and B' vs. Fig. 3A and A') and vice versa (Fig. 3C and C' vs. Fig. 2D and D'). This demonstrates the regulatory power of the Mlph adaptor protein over the MyoVa motor, irrespective of evolutionary origin. Such regulatory dominance suggests that the C-terminal FBD of the Mlph adaptor protein may represent a functionally dominant “command center” for cross-talk regulation.

To assess the cell-wide impact of Mlph-mediated track selection, we turned to computational modeling to simulate the dynamic redistribution of melanosomes as illustrated in Fig. 1B. Specifically, we addressed the following questions. Are the experimentally determined switching probabilities from our reconstitution assays capable of mediating any significant redistribution of these organelles on the cellular scale? If so, is there a specific functional purpose for regulating switching from actin filaments onto microtubules ($p_{AF \rightarrow MT}$) but not the reverse direction ($p_{MT \rightarrow AF}$), as observed in our assays (Fig. 3A vs. Fig. 3A')?

Simulation of Melanosome Motion in Amphibian Melanophores. To simulate the stochastic motion of melanosomes on a cell-wide scale, we developed a computational model as illustrated in Fig. 4 (see *SI Appendix* for details on the model and the impact of filament length, density, and distribution as well as dwell times of melanosomes on microtubule and actin filaments on simulated melanosome redistribution, *SI Appendix*, Figs. S6–S9). Because our aim was to translate the switching behavior of individual melanosomes at a single filament crossing to the intracellular organization of these organelles, we explicitly modeled cytoskeletal networks composed of individual actin and microtubule filaments. Such explicit modeling of filament networks has recently unmasked previously inaccessible theoretical aspects of intracellular transport (25–31), while effective, continuous models yielded first fundamental insights into cytoskeleton-dependent transport processes (32–36). In order to study the impact of interfilament switching on intracellular melanosome distribution in *Xenopus* melanophores, we varied the switching probabilities only, leaving the velocities of simulated melanosomes on the microtubule and actin networks unchanged. Specifically, we set the motility of melanosomes on microtubules to a constant, minus-end-directed velocity corresponding to the dynein-dominated activity that clusters melanosomes in *Xenopus* melanophores (37) (Fig. 1B, Right), as detailed in *SI Appendix*. We chose this implementation for two reasons. First, it represents the “worst-case” scenario for our interrogation of whether regulation of switching probabilities alone would suffice to reversibly distribute melanosomes throughout the cell (i.e., explicitly without regulating the microtubule-based motion). Second, it is well known that in amphibian melanophores, depolymerization of the actin network aggregates melanosomes at the minus ends of microtubules, even if the organelles were initially dispersed throughout the cell (37, 38).

Regulation of Switching Alone Prompts Redistribution of Melanosomes in Virtual Melanophore Cells. One intriguing finding obtained with the *Xenopus* model was that the switching probabilities from actin filaments onto microtubules ($p_{AF \rightarrow MT}$) were phosphorylation-dependent, while the switching probabilities from microtubules

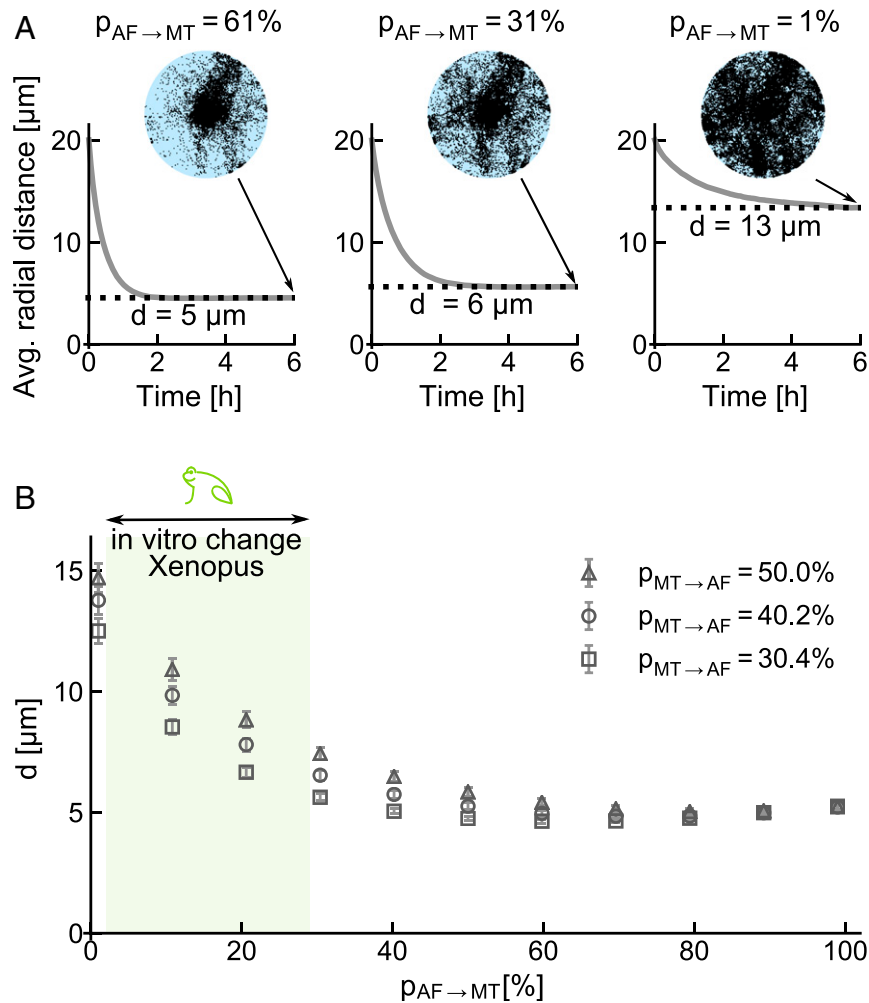


Fig. 5. Changes in $p_{AF \rightarrow MT}$ alone are sufficient to enable redistribution of melanosomes in virtual melanophores. (A) In our computer simulations, a continuous decrease of $p_{AF \rightarrow MT}$ suffices to darken the appearance of the virtual melanophores (top portion, left to right). Each average distance of melanosomes (avg. radial distance) from the cell center at a specific $p_{AF \rightarrow MT}$ approaches a stationary value d over time. This value quantifies how broadly melanosomes are dispersed throughout the cell (bottom portion depicts increasing values from left to right). As initial conditions we chose a homogeneous distribution of melanosomes throughout the cell. (B) The values for d obtained from simulations based on the computational model vary considerably within the range of experimentally determined $p_{AF \rightarrow MT}$ values (shaded area) for the *Xenopus* complex (2 to 29%, Fig. 3A' Phos. vs. Dephos.). In contrast, perturbations of $p_{MT \rightarrow AF}$ close to the value determined for the *Xenopus* transport complex ($\sim 46\%$, Fig. 3A) have only minor effects on d . Data correspond to an average over 35 cytoskeletal networks. Error bars reflect the SEM. Refer to *SI Appendix* for further details. AF, actin; MT, microtubule.

onto actin filaments ($p_{MT \rightarrow AF}$) were unregulated (Fig. 3A vs. Fig. 3A'). We therefore first investigated whether up-regulation of $p_{AF \rightarrow MT}$ impacts the melanosome distribution per se. As expected, a strong switching bias toward microtubules (large $p_{AF \rightarrow MT}$) led to clustering of melanosomes in the cell center (Fig. 5A, Left). Strikingly, however, our computer simulations showed that reducing $p_{AF \rightarrow MT}$ alone was sufficient to disperse the melanosomes throughout the cell (Fig. 5A, Middle and Right and Movies S4 and S5). There was no need to additionally down-regulate the minus-end bias of melanosome motion (i.e., the dynein-dependent motion; see Fig. 1B, Right) on the microtubules.

To quantify the extent of melanosome dispersion throughout the virtual melanophores with a single number, we used the average stationary distance d of melanosomes to the cell center. Put simply, large values of d correspond to a broad distribution of melanosomes throughout the whole cell, while d decreases with the degree of clustering in the cell center (Fig. 5A). For each melanophore and each set of switching probabilities, $p_{AF \rightarrow MT}$ and

$p_{MT \rightarrow AF}$, d approached a (unique) stationary value over time (Fig. 5B).

We then investigated the impact of the experimentally determined switching probabilities on the degree of melanosome dispersion throughout the cell as quantified by d . Remarkably, a systematic analysis of this parameter over the full range of $p_{AF \rightarrow MT}$ showed that varying this switching probability changes d most substantially within the range of the experimentally determined values (Fig. 3A' Phos. vs. Dephos., Fig. 5B, shaded area, and *SI Appendix*, Fig. S5). In fact, beyond these values, d did not change considerably as a response to variations of $p_{AF \rightarrow MT}$. These analyses thus support our hypothesis that solely regulating the switching of the *Xenopus* complex from actin onto microtubules, as reconstituted in our assays, may alone be sufficient to cause cell-wide melanosome redistribution (Fig. 5A). However, in contrast to variations of $p_{AF \rightarrow MT}$, even comparatively strong perturbations of $p_{MT \rightarrow AF}$ close to the experimentally determined probabilities failed to have any substantial effect on the degree of melanosome dispersion throughout the cell (Fig. 5B).

Taken together, our simulations support the notion that regulation of $p_{AF \rightarrow MT}$ alone would indeed provide a robust and efficient means to regulate the reorganization of melanosomes on a cell-wide scale. While additional regulation of microtubule-associated motors may support rapid transitions between dispersion and aggregation of melanosomes in vivo (Fig. 1 B, *Left vs. Right*), our simulations show that it is per se not required and that it can be compensated by solely regulating the cytoskeletal cross-talk (Movie S5 and *SI Appendix*, Fig. S5).

Regulation of $p_{AF \rightarrow MT}$ but Not $p_{MT \rightarrow AF}$ Affects Global Melanosome Redistribution. As described above, variation of $p_{MT \rightarrow AF}$ around the experimentally determined value of $\sim 46\%$ did not have any substantial impact on the degree of dispersion (Fig. 5B). We therefore wondered whether changes in the switching from microtubules onto actin filaments ($p_{MT \rightarrow AF}$) can prompt any relevant redistribution of melanosomes at all. To this end, we systematically evaluated changes in d over the full range of possible values for $p_{AF \rightarrow MT}$ and $p_{MT \rightarrow AF}$ to obtain a complete relation $d(p_{MT \rightarrow AF}, p_{AF \rightarrow MT})$ for any arbitrary pair of values (Fig. 6A; see *SI Appendix* for details). The result confirmed that the degree of melanosome distribution d is largely unresponsive to changes of $p_{MT \rightarrow AF}$ (Fig. 6A, red vs. yellow arrows). To quantitatively demarcate the functionally relevant range in which the melanosomes can be redistributed effectively by changing either $p_{AF \rightarrow MT}$ or $p_{MT \rightarrow AF}$, we determined the regulatory sensitivities of $d(p_{MT \rightarrow AF}, p_{AF \rightarrow MT})$ with respect to such variations. Specifically, regulatory sensitivity was computed as the magnitude of the slope of $d(p_{MT \rightarrow AF}, p_{AF \rightarrow MT})$. As indicated in Fig. 6B, the regions of sensitive regulation by changes of $p_{MT \rightarrow AF}$ was much more limited compared to $p_{AF \rightarrow MT}$. Strikingly, the region of switching probabilities that is irrelevant for an effective regulation in virtual melanophores covers the experimentally determined (unregulated) probabilities of the zebrafish and *Xenopus* complexes to switch from microtubules onto actin (Fig. 6 B, *Right*). In stark contrast to the unregulated $p_{MT \rightarrow AF}$ (Fig. 3A, Phos. vs. Dephos.), the regulated $p_{AF \rightarrow MT}$ as displayed by the *Xenopus* complex (Fig. 3A', Phos. vs. Dephos.) was positioned well within the regulatory-sensitive region (Fig. 6B, *Left*, black arrow).

Taken together, our computational model provides a compelling rationale for two aspects of our experimental findings. First, by demarcating the regime of most efficient organelle redistribution in virtual melanophores, our simulations underline the functional significance of regulating the switching from actin onto microtubules, but not the other way around, to enforce cross-talk (Fig. 3A vs. Fig. 3A'). Second, the striking agreement between the experimentally determined magnitudes of switching probabilities (Fig. 3A', Phos. vs. Dephos.) and the range of regulatory sensitivity that is predicted by our computational model (Fig. 6) provides strong support that regulation of cross-talk alone would in principle be sufficient to efficiently and reversibly redistribute melanosomes on a cell-wide scale (Fig. 1B).

Together with our previous dissection of the mammalian model (9), we have unmasked an intriguing trajectory of how cross-talk may have been established through evolution. While *DrMlph* proteins from the early vertebrate zebrafish cannot regulate switching in either direction, the amphibian *XlMlph* acquired the ability to up-regulate the switching of its *XlMyoVa* motor from actin filaments onto microtubules. The mammalian *MmMlph*, on the other hand, is capable of up-regulating both, switching onto microtubules and switching onto actin filaments (9). We plotted a simple phylogenetic tree to assess whether the evolutionary relationships between the *Mlph* sequences and the respective organisms correlate (*SI Appendix*, Fig. S10). As expected and consistent with

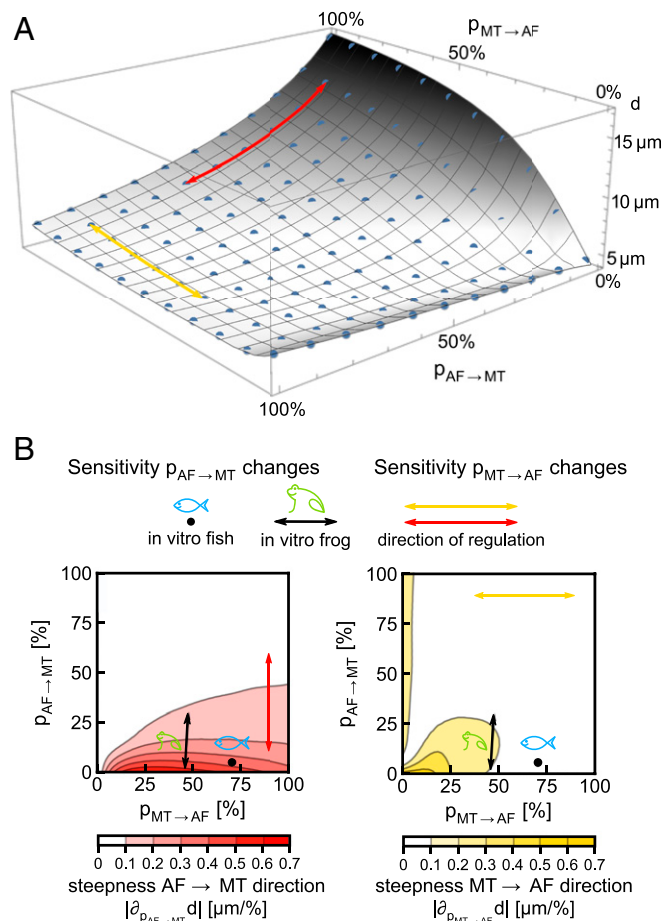


Fig. 6. Degree of melanosome dispersion throughout a cell is regulated efficiently by changing the switching probability from actin filaments to microtubules ($p_{AF \rightarrow MT}$) but not by altering the switching probability in the reverse direction ($p_{MT \rightarrow AF}$). (A) The degree of melanosome dispersion d throughout the cell was determined for 121 pairs of values for $p_{AF \rightarrow MT}$ and $p_{MT \rightarrow AF}$ (closed symbols). Each of the data points corresponds to an ensemble average over 35 cytoskeletal networks. We interpolated these data points with a two-dimensional spline (gray surface) to obtain a functional relation $d(p_{MT \rightarrow AF}, p_{AF \rightarrow MT})$ over the full range of possible values for the switching probabilities. The shading of the surface indicates whether a virtual melanophore would appear dark or bright. (B) Regulatory sensitivity as quantified by the magnitudes of the slopes in the respective directions. Regulatory sensitivity (dark-colored areas) is substantially more pronounced for changes in $p_{AF \rightarrow MT}$ than $p_{MT \rightarrow AF}$. Red and yellow arrows indicate changes in the $p_{AF \rightarrow MT}$ and $p_{MT \rightarrow AF}$ direction, respectively, and are located at the same positions in A and B to guide the eye. The black arrow refers to experimentally determined switching probabilities of the *Xenopus* complex shown in Fig. 3 A and A'. The black point is located at the switching probabilities determined for zebrafish complexes (Fig. 2 A and A' and *SI Appendix*, Fig. S3 B–C). For details, refer to *SI Appendix*. AF, actin; MT, microtubule.

previous reports (21, 39), a gene duplication occurred in the fish lineage leading to multiple *Mlph* proteins in fish but not in land animals or amphibians. Furthermore, the evolutionary relationships between the *Mlph* proteins correlated with the relationships between the organisms.

What might be the mechanistic rationale for the up-regulated switching of the actin-associated *XlMyoVa* motor onto microtubules in the amphibian model? Our systematic mechanistic dissection now provides a straightforward, simple explanation. We find that up-regulation alone is fully sufficient for a cell-wide redistribution of melanosomes in silico (Fig. 5 and Movies S4 and S5), which mediates physiological color change in vivo (1, 20).

As such, a microscopic parameter (switching probabilities between filaments) dictates the collective behavior of melanosomes, which leads to a macroscopically observed change in phenotype.

The failure of zebrafish *DrMlph* proteins to regulate any switching probabilities of their *DrMyoVa* motor (Fig. 2 *A* and *A'* and *SI Appendix*, Fig. S3 *B–C'*), on the other hand, provokes the question of whether the *MyoVa*/actin system is involved in a regulated cross-talk between the microtubule and actin networks in the fish model. Indeed, the most conspicuous difference between fish and amphibians is the use of the actin system. It is long established that in the absence of the actin network the microtubule system alone is sufficient to ensure redistribution of melanosomes in the fish model (40). In stark contrast, removal of the actin network in amphibian melanophores prevents such cell-wide redistribution, and melanosomes cluster irreversibly in the cell center (38). The latter underscores the necessity of both, the actin and microtubule systems, in reversible melanosome redistribution to bring about a physiological color change in the amphibian model (Fig. 1*B*). In line with these observations, we have been able to reconstitute regulated cross-talk at microtubule–actin crossings with the amphibian but not the zebrafish model in vitro (Fig. 2 *A* and *A'* vs. Fig. 3 *A* and *A'*).

Based on our systematic dissection and previous in vivo findings described above, we therefore propose that in the fish model regulated cross-talk between the microtubule and actin network systems via the *MyoVa*/actin is not yet evolved, whereas cross-talk in the amphibian model is required to ensure cell-wide redistribution of melanosomes for physiological color change in vivo. We provide a molecular explanation for the specific regulation of the switching from actin filaments onto microtubules and demonstrate that switching in the opposite direction is insufficient to regulate the redistribution of melanosomes (Fig. 6*B*). In agreement with our proposed model, previous in vivo

studies on intact melanosomes suggested that the switching of melanosomes onto the actin network is not regulated in fish melanophores (32).

Two aspects of our systematic mechanistic dissection of *Mlph*-mediated cross-talk deserve further scrutiny in the future. Can functional cross-talk be engineered into zebrafish in vivo as we demonstrate here in vitro? Furthermore, why does the mammalian model regulate switching probabilities even though cross-talk appears to be irrelevant for physiological color change (4)? Last but not least, given that the vast majority of myosin, kinesin, and dynein motors are recruited to their designated cargo via adaptor proteins, it will be interesting to see if other adaptors interfere with the motor-dependent transport regulation in a way similar to that observed for *Mlph*.

Data Availability. All data that support the findings of this study are available within the paper and *SI Appendix*. Custom-written codes used in this study are available from the corresponding authors upon reasonable request.

ACKNOWLEDGMENTS. We thank Stefani Spranger (Massachusetts Institute of Technology, Cambridge, MA) for extracting mRNA from *Xenopus laevis* melanophores and providing us with the complementary DNA; Nagarjuna Nagaraj (Max Planck Institute for Biochemistry Core Facility, Martinsried, Germany) for the mass spectrometry analyses; Vladimir I. Gelfand (Northwestern University, Chicago) for his generous gift of melanophore culture; Vladimir I. Gelfand (Northwestern University, Chicago) and Minjong Park (University of California, San Francisco) for the *XtMlph* plasmid; Günther Woehlke (Technische Universität München, Munich) for fruitful discussions on the project; and our anonymous referees for their critical input that significantly improved the manuscript and the strength of its conclusions, and in particular the phylogenetic tree that supports our proposed molecular model. This work was funded by Deutsche Forschungsgemeinschaft grant SFB-863, project ID 111166240. Z.Ö. acknowledges a starting grant from the European Research Council (GA 335623). E.F. acknowledges hospitality at the Kavli Institute of Nanoscience at TU Delft where part of this work was done.

1. S. Aspöngren, D. Hedberg, H. N. Skold, M. Wallin, "New insights into melanosome transport in vertebrate pigment cells" in *International Review of Cell and Molecular Biology*, K. W. Jeon, G. H. Bourne, J. Jarvik, J. F. Danielli, M. Friedlander, Eds. (Elsevier, 2009), vol. 272, pp. 245–302.
2. M. W. Elting, P. Suresh, S. Dumont, The spindle: Integrating architecture and mechanics across scales. *Trends Cell Biol.* **28**, 896–910 (2018).
3. F. Huber, A. Boire, M. P. López, G. H. Koenderink, Cytoskeletal crosstalk: When three different personalities team up. *Curr. Opin. Cell Biol.* **32**, 39–47 (2015).
4. A. N. Hume, M. C. Seabra, Melanosomes on the move: A model to understand organelle dynamics. *Biochem. Soc. Trans.* **39**, 1191–1196 (2011).
5. E. E. Joo, K. M. Yamada, Post-polymerization crosstalk between the actin cytoskeleton and microtubule network. *Bioarchitecture* **6**, 53–59 (2016).
6. M. Dogterom, G. H. Koenderink, Actin-microtubule crosstalk in cell biology. *Nat. Rev. Mol. Cell Biol.* **20**, 38–54 (2019).
7. A. Elie et al., Tau co-organizes dynamic microtubule and actin networks. *Sci. Rep.* **5**, 9964 (2015).
8. M. Kwon, M. Bagonis, G. Danuser, D. Pellman, Direct microtubule-binding by myosin-10 orients centrosomes toward retraction fibers and subcortical actin clouds. *Dev. Cell* **34**, 323–337 (2015).
9. A. Oberhofer et al., Myosin Va's adaptor protein melanophilin enforces track selection on the microtubule and actin networks in vitro. *Proc. Natl. Acad. Sci. U.S.A.* **114**, E4714–E4723 (2017).
10. M. A. A. Mohamed, W. L. Stepp, Z. Ökten, Reconstitution reveals motor activation for intraflagellar transport. *Nature* **557**, 387–391 (2018).
11. M. Fukuda, T. S. Kuroda, Slac2-c (synaptotagmin-like protein homologue lacking C2 domains-c), a novel linker protein that interacts with Rab27, myosin Va/Vila, and actin. *J. Biol. Chem.* **277**, 43096–43103 (2002).
12. A. N. Hume et al., The leaden gene product is required with Rab27a to recruit myosin Va to melanosomes in melanocytes. *Traffic* **3**, 193–202 (2002).
13. L. E. Matesic et al., Mutations in *Mlph*, encoding a member of the Rab effector family, cause the melanosome transport defects observed in leaden mice. *Proc. Natl. Acad. Sci. U.S.A.* **98**, 10238–10243 (2001).
14. K. Nagashima et al., Melanophilin directly links Rab27a and myosin Va through its distinct coiled-coil regions. *FEBS Lett.* **517**, 233–238 (2002).
15. D. W. Provance, T. L. James, J. A. Mercer, Melanophilin, the product of the leaden locus, is required for targeting of myosin-Va to melanosomes. *Traffic* **3**, 124–132 (2002).
16. X. S. Wu et al., Identification of an organelle receptor for myosin-Va. *Nat. Cell Biol.* **4**, 271–278 (2002).
17. T. S. Kuroda, H. Ariga, M. Fukuda, The actin-binding domain of Slac2-a/melanophilin is required for melanosome distribution in melanocytes. *Mol. Cell. Biol.* **23**, 5245–5255 (2003).
18. M. Skolnick, E. B. Kremensova, D. M. Warshaw, K. M. Trybus, More than just a cargo adapter, melanophilin prolongs and slows processive runs of myosin Va. *J. Biol. Chem.* **288**, 29313–29322 (2013).
19. A. Daniolos, A. B. Lerner, M. R. Lerner, Action of light on frog pigment cells in culture. *Pigm. Cell Res.* **3**, 38–43 (1990).
20. A. A. Nascimento, J. T. Roland, V. I. Gelfand, Pigment cells: A model for the study of organelle transport. *Annu. Rev. Cell Dev. Biol.* **19**, 469–491 (2003).
21. L. Sheets, D. G. Ransom, E. M. Mellgren, S. L. Johnson, B. J. Schnapp, Zebrafish melanophilin facilitates melanosome dispersion by regulating dynein. *Curr. Biol.* **17**, 1721–1734 (2007).
22. A. D. Mehta et al., Myosin-V is a processive actin-based motor. *Nature* **400**, 590–593 (1999).
23. M. Y. Ali et al., Myosin Va maneuvers through actin intersections and diffuses along microtubules. *Proc. Natl. Acad. Sci. U.S.A.* **104**, 4332–4336 (2007).
24. D. Zimmermann, B. Abdel Motaal, L. Voith von Voithenberg, M. Schliwa, Z. Ökten, Diffusion of myosin V on microtubules: A fine-tuned interaction for which E-hooks are dispensable. *PLoS One* **6**, e25473 (2011).
25. D. Ando, N. Korabel, K. C. Huang, A. Gopinathan, Cytoskeletal network morphology regulates intracellular transport dynamics. *Biophys. J.* **109**, 1574–1582 (2015).
26. J. Snider et al., Intracellular actin-based transport: How far you go depends on how often you switch. *Proc. Natl. Acad. Sci. U.S.A.* **101**, 13204–13209 (2004).
27. A. Kahana, G. Kenan, M. Feingold, M. Elbaum, R. Granek, Active transport on disordered microtubule networks: The generalized random velocity model. *Phys. Rev. E Stat. Nonlin. Soft Matter Phys.* **78**, 051912 (2008).
28. B. Embley, A. Parmeggiani, N. Kern, Understanding totally asymmetric simple-exclusion-process transport on networks: Generic analysis via effective rates and explicit vertices. *Phys. Rev. E Stat. Nonlin. Soft Matter Phys.* **80**, 041128 (2009).
29. P. J. Mlynarczyk, S. M. Abel, First passage of molecular motors on networks of cytoskeletal filaments. *Phys. Rev. E* **99**, 022406 (2019).
30. I. Neri, N. Kern, A. Parmeggiani, Totally asymmetric simple exclusion process on networks. *Phys. Rev. Lett.* **107**, 068702 (2011).

31. I. Neri, N. Kern, A. Parmeggiani, Exclusion processes on networks as models for cytoskeletal transport. *New J. Phys.* **15**, 085005 (2013).
32. B. M. Slepchenko, I. Semenova, I. Zaliapin, V. Rodionov, Switching of membrane organelles between cytoskeletal transport systems is determined by regulation of the microtubule-based transport. *J. Cell Biol.* **179**, 635–641 (2007).
33. C. Loverdo, O. Bénichou, M. Moreau, R. Voituriez, Enhanced reaction kinetics in biological cells. *Nat. Phys.* **4**, 134–137 (2008).
34. P. C. Bressloff, J. M. Newby, Stochastic models of intracellular transport. *Rev. Mod. Phys.* **85**, 135–196 (2013).
35. A. E. Hafner, H. Rieger, Spatial cytoskeleton organization supports targeted intracellular transport. *Biophys. J.* **114**, 1420–1432 (2018).
36. A.-T. Dinh, T. Theofanous, S. Mitragotri, Modeling of pattern regulation in melanophores. *J. Theor. Biol.* **244**, 141–153 (2007).
37. S. P. Gross et al., Interactions and regulation of molecular motors in *Xenopus* melanophores. *J. Cell Biol.* **156**, 855–865 (2002).
38. S. L. Rogers, V. I. Gelfand, Myosin cooperates with microtubule motors during organelle transport in melanophores. *Curr. Biol.* **8**, 161–164 (1998).
39. S. M. K. Glasauer, S. C. F. Neuhauss, Whole-genome duplication in teleost fishes and its evolutionary consequences. *Mol. Genet. Genomics* **289**, 1045–1060 (2014).
40. V. I. Rodionov, A. J. Hope, T. M. Svitkina, G. G. Borisy, Functional coordination of microtubule-based and actin-based motility in melanophores. *Curr. Biol.* **8**, 165–168 (1998).